Hindawi
Discrete Dynamics in Nature and Society
Volume 2023, Article ID 7273140, 14 pages
https://doi.org/10.1155/2023/7273140

Research Article

An Impulse-Quantizing Synchronization Approach for Mixed Continuous-Discrete Complex Networks

Na Hu, Luyan Li, Honghua Bin, and Zhenkun Huang

School of Science, Jimei University, Xiamen 361021, China

Correspondence should be addressed to Zhenkun Huang; hzk974226@jmu.edu.cn

Received 19 October 2022; Revised 4 April 2023; Accepted 29 September 2023; Published 13 October 2023

Academic Editor: Ya Jia

This paper presents synchronization of mixed continuous-discrete complex network via impulse-quantizing approach. A delay-partitioning group strategy is proposed and impulse-quantizing control is designed to derive theoretical criteria ensuring scale-type synchronization of complex networks. Our results show that synchronization of mixed continuous-discrete complex networks can be realized by controlling delay-partitioning subgroup nodes with impulsive quantization. The theoretical results give scale-limited sufficient conditions for quantized synchronization relying on control gains, impulsive intervals, and delays. A numerical simulation is given to demonstrate the effectiveness of the theoretical results.

1. Introduction

A complex network is a dynamical system composed of a large number of nodes with various interconnection and active interaction. Since complex networks have intrinsic characteristics of dynamic evolution, connection diversity, and structural complexity, many researchers from different disciplines have paid increasing attention to complex networks in the past few decades [1–3]. Meanwhile, the synchronization control of complex networks has been extensively studied due to its broad and cross-border applications in the fields of social networks, power grids, digital encryption communications, brain science, electronics, and so on [4]. By synthetically employing the control theory, various synchronization control strategies have been implemented for complex networks [5–9].

In recent ten years, many scholars have obtained a large number of constructive results on the synchronization of complex networks, and put forward many effective methods, such as feedback control [10], pinning control [11, 12], and impulsive control [13]. In fact, in the real world, there are often interference factors such as channel congestion, frequency change, and delays [14, 15]. Therefore, it is important to focus on the interactions of nodes in complex networks. In [16], the authors proposed that a complex network can be considered as the composition system with the two coupled dynamic subsystems: the nodes subsystem (NS) and the links subsystem (LS). The links synchronization is defined and synthesizes the adaptive control scheme to realize it. In [17], the authors described the dynamic behaviour of LS with the outgoing links vector at every node, and a double tracking control for the directed complex dynamic network via the state observer of outgoing links is presented. Coupling configurations between network nodes will have impulsive discontinuity, that is, the topology of the network is dynamic and may subject to instantaneous transmission. In [18], finite-time synchronization problem of uncertain nonlinear complex networks with time-varying delay is studied.

The traditional synchronous control often relies on the state or output feedback continuous signal, but in reality, the control system is based on digital equipment such as computers with limited accuracy. The signals between network nodes and controllers are transmitted through the network with limited capacity, and the feedback control signal usually needs to be quantified before transmission [19–24]. The quantization errors will affect the synchronization of the network. In [25], quantization and cyclic protocols are used to solve the problem of limited communication channel capacity, and then intermittent control strategy is used to improve the efficiency of communication channel and controller. In [26], quantization and trigger errors are combined to discuss the synchronization of Lur'e form driven response system in finite channel. Due to the solution, space of the high-dimensional dynamic system described by the dynamic network with quantized signal is more complex than the general continuous or discrete dynamic system, and its theoretical analysis is also more attractive and challenging.

However, in many network systems, the interaction among subsystems would occur at any different time domains including discrete-time sequences or continuous time intervals, respectively [27, 28]. To avoid adopting separate dynamical analysis, it makes sense to discuss these systems on time scales [28, 29] which can unify continuous and discrete dynamics under a unified framework. In [30], based on the time scale theory of calculus and linear matrix inequality (LMI), some sufficient conditions are obtained to ensure the global synchronization of the complex networks with delays. In [31], the synchronization problem of linear dynamical networks on time scale was deal through node-based pinning control. Inspired by existing ones [31–33], we incorporate impulse-quantizing control strategy into complex networks and discuss scale-type synchronization on time scales.

The novelty of our contribution is three-fold, which is shown as follows:

(1) Unlike the existing traditional quantized control [19–24], we propose a delay-partitioning group strategy and impulse-quantizing controller to achieve complex network synchronization, which can better reduce signal transmission burden and decrease control costs.

(2) Owning to breaking the limitation of studying discrete and continuous systems [27, 28] separately, new synchronization criteria for mixed continuous-discrete complex networks relying on control gains, impulsive intervals, and delays are derived.

(3) It is the first time that a flexible impulse-quantizing controller is discussed in mixed continuous-discrete complex networks [34]. The proposed method provides a framework for synchronization of mixed continuous-discrete complex network with quantized impulses.

The main structure of this paper is as follows. In Section 2, we introduce some basic theories and present the quantized synchronization problem of mixed continuous-discrete complex networks. In Section 3, quantization scale-synchronization criteria of complex networks are established. In Section 4, the effectiveness of the proposed control strategy is illustrated by numerical simulations. Finally, Section 5 summarizes this paper.

2. Preliminaries and Model

In this section, we give some basic definitions and related Lemmas about time scale. For the theory of time scale, we refer to the monograph [35].

Let T be a time scale (i.e., a nonempty closed subset of R). The forward jump operator $\sigma\colon \mathrm{T} \longrightarrow \mathrm{T}$ is defined by $\sigma(t)\colon = \inf\{s \in \mathrm{T}\colon s > t\}$ for all $t \in \mathrm{T}$, while the backward jump operator $\rho\colon \mathrm{T} \longrightarrow \mathrm{T}$ is defined by $\rho(t)\colon = \sup\{s \in \mathrm{T}\colon s < t\}$ for all $t \in \mathrm{T}$. If $\sigma(t) > t$, we say that t is right-scattered, while if $\rho(t) < t$ we say that t is left-scattered. Also, if $\sigma(t) = t$, we say that t is right-dense, while if $\rho(t) = t$ we say that t is left-dense. Define $\mathrm{T}^{\kappa} = \mathrm{T} - \{M\}$, when T has a left-scattered maximum M, otherwise $\mathrm{T}^{\kappa} = \mathrm{T}$. The graininess function $\mu\colon \mathrm{T} \longrightarrow [0,\infty)$ is defined by $\mu(t) = \sigma(t) - t$.

Definition 1 (see [35]). Let $f\colon \mathrm{T} \longrightarrow \mathrm{R}$ and $t \in \mathrm{T}^{\kappa}$. $f^{\Delta}(t)$ is said to be the delta derivative of f at t, given any $\varepsilon > 0$, if there is a neighborhood U of t such that

$$\left| f(\sigma(t)) - f(s) - f^{\Delta}(\sigma(t) - s) \right| \leq \varepsilon |\sigma(t) - s|. \tag{1}$$

Definition 2 (see [35]). A function $f\colon \mathrm{T} \longrightarrow \mathrm{R}$ is rd-continuous if it is continuous at right-dense points in T and its left-sided limits exist at left-dense points in T. The set of all rd-continuous functions $f\colon \mathrm{T} \longrightarrow \mathrm{R}$ will be denoted by C_{rd}. A function $p\colon \mathrm{T} \longrightarrow \mathrm{R}$ is regressive provided $1 + \mu(t)p(t) \neq 0$ for all $\in \mathrm{T}^{\kappa}$. Denote by $\mathfrak{R}$ the set of all regressive, rd-continuous functions $f\colon \mathrm{T} \longrightarrow \mathrm{R}$ and $\mathfrak{R}^{+}\colon = \{p \in \mathfrak{R}\colon 1 + \mu(t)p(t) > 0, \forall t \in T\}$.

Definition 3 (see [35]). If $p \in \mathfrak{R}$, the exponential function $e_p(t,s)\colon = \exp\left(\int_s^t \xi_{\mu(t)}(p(\tau))\Delta\tau\right)$ for $t, s \in \mathrm{T}$, where the cylinder transformation $\xi_h(z) = \begin{cases} \log(1 + hz)/h, & h \neq 0 \\ z, & h = 0 \end{cases}$ and Log is the natural logarithm function.

Remark 4. Let $\alpha \in \mathfrak{R}$ be constant. If $\mathrm{T} = \mathrm{Z}$, then $e_{\alpha}(t,t_0) = (1+\alpha)^{t-t_0}$ for all $t \in \mathrm{T}$. If $\mathrm{T} = \mathrm{R}$, then $e_{\alpha}(t,t_0) = e^{\alpha(t-t_0)}$ for all $t \in \mathrm{T}$. If $\alpha \geq 0$, then $e_{\alpha}(t,s) \geq 1$ for $t \geq s$ and $t, s \in \mathrm{T}$.

Lemma 5 (see [35]). *If* $f \in C_{rd}$ *and* $\in \mathrm{T}^{\kappa}$, *then* $\int_t^{\sigma(t)} f(\tau)\Delta\tau = \mu(t) f(t)$.

Lemma 6 (see [35]). *Let* $f \in C_{rd}$ *and* $p \in \mathfrak{R}$. *For all* $t \in \mathrm{T}$, *the dynamic inequality* $y^{\Delta}(t) \leq p(t)y(t) + f(t)$ *implies that* $y(t) \leq y(t_0)e_p(t,t_0) + \int_{t_0}^{t} e_p(t,\sigma(\tau)) f(\tau)\Delta\tau$.

Let R^n be the n-dimensional Euclidean space with norm $\|\cdot\|$. Let Z^{+} denote the set of positive integer numbers, N is the set of natural numbers, $\mathrm{R}^{n\times n}$ is the set of all $n \times n$ real matrices. The superscript T stands for the transpose of a matrix. I is an appropriately dimensioned identity matrix. The notion $X \geq Y$ (respectively, $X \geq Y$) means that the matrix $X - Y$ is positive semidefinite (respectively, positive definite).

Lemma 7 (see [35]). *If* $p \in \mathfrak{R}$, $c \in \mathrm{T}$, *and* $f, g\colon \mathrm{T} \longrightarrow \mathrm{R}$ *are differentiable at* $t \in \mathrm{T}^{\kappa}$, *then*

$$\begin{aligned} \left[e_p(c,\cdot)\right]^{\Delta} &= -p\left[e_p(c,\cdot)\right]^{\sigma}, \\ (fg)^{\Delta}(t) &= f^{\Delta}(t)g(t) + f(\sigma(t))g^{\Delta}(t) \\ &= f(t)g^{\Delta}(t) + f^{\Delta}(t)g(\sigma(t)). \end{aligned} \tag{2}$$

In this paper, assume that Q: R $\longrightarrow$ R is a logarithmic quantization function, the set of logarithmic quantization levels is described by the following equation:

$$U := \left\{ \pm u_i, u_i = \rho^i u_0, i = \pm 1, \pm 2, \cdots \right\} \cup \left\{ \pm u_0 \right\} \cup \{0\}, 0 < \rho < 1, u_0 > 0. \tag{3}$$

The associated quantizer is defined as follows:

$$Q(a) = \begin{cases} u_i, & \text{if } \dfrac{1}{1+\delta} u_i < a \leq \dfrac{1}{1-\delta} u_i, a > 0, \\ 0, & \text{if } a = 0, \\ -Q(-a), & \text{if } a < 0, \end{cases} \tag{4}$$

where $\delta = (1-p)/(1+p)$ and $Q(a) = (1+\Theta)a$ with $\Theta \in [-\mathcal{S}, \mathcal{S}]$.

Consider the following mixed continuous-discrete complex dynamic networks (CDNs) with N identical nodes on time scale T as follows:

$$x_i^{\Delta}(t) = A x_i(t) + B f(x_i(t)) + c \sum_{j=1}^{N} g_{ij} \Gamma x_j(t), i = 1, 2, \ldots, N, \tag{5}$$

where $x_i(t) \in \mathrm{R}^n$ denotes the state vector of the i th node, $c > 0$ is the coupling strength, $f(x_i(t)) = \Big(f_1(x_{i1}(t)), f_2(x_{i2}(t)), \cdots, f_n(x_{in}(t)) \Big)^T$ is a nonlinear function, $A, B \in \mathrm{R}^{n \times n}$ are constant matrices, $G = (g_{ij})_{N \times N}$ represents the network connection topology, which is defined as follows: if there is a connection between the i th node and the j th node $(i \neq j)$, then $g_{ij} = g_{ji} = 1$; otherwise, $g_{ij} = g_{ji} = 0$, and the diagonal elements are defined as $g_{ii} = -\sum_{j=1, j\neq i}^{N} g_{ij}$. $\Gamma = \mathrm{diag}\ \{\gamma_1, \gamma_2, \cdots, \gamma_n\} > 0$ is the inner coupling matrix between nodes. For system (5), we introduce an isolated node as synchronization target, which is described as follows:

$$y^{\Delta}(t) = A y(t) + B f(y(t)), \tag{6}$$

where $y(t) = \left(y_1(t), y_2(t), \cdots y_n(t) \right)^T$ and $f(y(t)) = \Big(f_1(y_1(t)), f_2(y_2(t)), \cdots f_n(y_n(t)) \Big)^T$.

Consider system (5) with feedback control as follows:

$$\begin{aligned} x_i^{\Delta}(t) &= A x_i(t) + B f(x_i(t)) \\ &\quad + c \sum_{j=1}^{N} g_{ij} \Gamma x_j(t) + u_i(t), i = 1, 2, \cdots, N, \end{aligned} \tag{7}$$

where the impulse-quantizing controller is designed as follows:

$$u_i(t) = \sum_{k=1}^{\infty} Q\big(q_j e_i(t) + q_j e_i(t) + \overline{q}_j e_i(t - \tau_j)\big) \delta(t - t_k). \quad i \in N_j. \tag{8}$$

Each $e_i(t) = x_i(t) - y(t)$ is an error vector of i th node, $\delta(\cdot)$ is the Dirac delta function, q_j and $\overline{q}_j$ are the designed impulsive control gain.

N_j denotes a delay-partitioning subgroup which allows τ_i-delay impulse imposed on all nodes in N_j, $N_1 \cup N_1 \cup \cdots \cup N_m = N$, and $N_i \cap N_j = \varnothing, i \neq j$. $\{t_k\}_{k=0}^{\infty} \subset$ T is a strictly increasing impulse sequence with $t_n \longrightarrow \infty$, $n \longrightarrow \infty$. There exists a constant $\tau > 0$ such that $\tau_j < \tau$ for all $j \in \{1, 2, \cdots, m\}$, the discrete sequence $\left\{t_k - \tau_j\right\}$ satisfies $t_i - \tau \geq t_0$ and $t_k - \tau_j \in$ T.

Then, system (7) can be described as follows:

$$\text{As } i \in N_j, \begin{cases} x_i^{\Delta}(t) = A x_i(t) + B f(x_i(t)) + c \displaystyle\sum_{j=1}^{N} g_{ij} \Gamma x_j(t), & t \neq t_k, \\ \Delta x_i(t) = Q\big(q_j e_i(t) + \overline{q}_j e_i(t - \tau_j)\big), & t = t_k, \end{cases} \tag{9}$$

where $\Delta x_i(t_k) = x_i(t_k^+) - x_i(t_k^-)$ and $x_i(t_k^-) - x_i(t_k)$.

From equations (6) and (9), one can get the following error system:

$$\text{As } i \in N_j, \begin{cases} e_i^{\Delta}(t) = Ae_i(t) + Bf(e_i(t)) + c\sum_{j=1}^{N} g_{ij}\Gamma e_j(t), & t \neq t_k, \\ \Delta e_i(t) = Q\left(q_j e_i(t) + \overline{q}_j e_i\left(t - \tau_j\right)\right), & t = t_k, \end{cases} \tag{10}$$

where $f(e_i(t)) = f(x_i(t)) - f(y(t))$.

Remark 8. Due to the limitation of network broadband, data transmission between nodes in networks will arouse delays [36] and needs to be quantified, and the quantization will affect the performance of the system [24, 32]. Therefore, an impulse-quantizing multigroup strategy is proposed for equation (9) and it has a very important impact on the system synchronization.

Definition 9. System (7) is said to achieve impulse-quantizing synchronization with system (6), if

$$\lim_{t \longrightarrow \infty} \left\| x_i(t) - y(t) \right\| = 0 \text{ for all } i = 1, 2, \cdots, N. \tag{11}$$

Lemma 10. *Given any vector x, y, a positive definite matrix H, and ε is a positive definite constant and satisfies $\varepsilon > 0$, then the following inequality holds:*

$$2x^T y \leq \varepsilon x^T H x + \varepsilon^{-1} y^T H^{-1} y. \tag{12}$$

In this paper, we always assume that each $f_i(\cdot)$ satisfies the Lipschitz condition, i.e., there exists a positive constant l_i, $(i = 1, 2, \cdots, n)$, such that $|f_i(x_1) - f_i(x_2)| \leq l_i |x_1 - x_2|$ holds for $x_1, x_2 \in \mathrm{R}$. For simplification, denote $L: = \mathrm{diag}\{l_1, l_2, \cdots, l_n\}$.

3. Main Results

In the section, we give some criteria for impulse-quantizing synchronization of system (5) with delayed impulses.

Theorem 11. *If there exist scalars $\alpha > 0, \nu > 0, \beta_i > 0$ $(i = 1, 2, 3), \varepsilon_i > 0 \, (i = 1, \cdots, m)$ and matrices $P^T = P > 0$, $Q_1 > 0$, and $Q_2 > 0$ satisfying the following inequalities, then*

$$\begin{aligned} (A_1)&: \left(G^T G\right) \otimes \left(\Gamma^T P \Gamma\right) \leq (\beta_1 I_N) \otimes P, \left(G^T G\right) \otimes \left(\Gamma^T A^T P \Gamma\right) \leq (\beta_2 I_N) \otimes \left(A^T P\right), \\ &\left(G^T G\right) \otimes \left(\Gamma^T B^T P \Gamma\right) \leq (\beta_3 I_N) \otimes \left(B^T P\right). \end{aligned} \tag{13}$$

$$(A_2): \begin{pmatrix} \Xi & PB & \sqrt{\mu} A^T PB \\ * & -Q_1 & 0 \\ * & * & -Q_2 \end{pmatrix} \leq 0, \tag{14}$$

where $\tilde{\Xi}: = \mu A^T PA + \mu L^T Q_2 L + c\mu L^T PBL + c\mu\left((cc\beta_1 + \beta_2 A^T + \beta_3 B^T)P + PA\right)$ *and* $\Xi: = A^T P + PA + c(1 + \beta_1)P + L^T Q_1 L + \tilde{\Xi} - \alpha P$. (A_3): $(d_M + \sum_{i=1}^{m} d_i e^{\nu\tau_i}) e^{\nu(t_{k+1} - t_k)} e_\alpha \;(t_{k+1}, t_k) \leq 1$, *where* $d_i = (1 + \varepsilon_i^{-1})(1 + \Theta)^2 \overline{q}_i^2, i = 1, 2, \cdots, m$ *and* $d_M = \max_{i \in \{1, \cdots, m\}} \left\{(1 + \varepsilon_i)\left((1 + \Theta) q_i + 1\right)^2\right\}$.

Then, system (9) can achieve impulse-quantizing synchronization with system (6).

Proof. Set $e(t) = (e_1{}^T(t), e_2{}^T(t), \cdots e_n{}^T(t))^T$ and $f(e(t)) = (f^T(e_1(t)), f^T(e_2(t)), \cdots, f^T(e_N(t)))^T$, then system (10) can be rewritten as follows:

$$\text{As } i \in N_j, \begin{cases} e^{\Delta}(t) = (I_N \otimes A)e(t) + (I_N \otimes B)f(e(t)) + c(G \otimes \Gamma)e(t), & t \neq t_k, \\ \Delta e_i(t) = Q\left(q_j e_i(t) + \overline{q}_j e_i\left(t - \tau_j\right)\right), & t = t_k. \end{cases} \tag{15}$$

Consider Lyapunov function $V(t) = e^T(t)(I_N \otimes P)e(t)$. Calculating the Δ-derivative of $V(t)$ over impulsive interval $t \in$, $k \in \mathrm{Z}_+$ along the trajectory of system (10), we get the following equation:

$$\begin{aligned}
V^{\Delta}(t) &= \sum_{i=1}^{N}\left[\left(e_i^T\right)^{\Delta} Pe_i + \left(e_i^T\right)^{\sigma} Pe_i^{\Delta}\right] \\
&= \sum_{i=1}^{N}\left[\left(e_i^T\right)^{\Delta} Pe_i + \left(e_i + \mu e_i^{\Delta}\right)^{T} Pe_i^{\Delta}\right] \\
&= \sum_{i=1}^{N}\Bigg[e_i^T\left(A^TP + PA + \mu A^TPA\right)e_i + 2e_i^TPBf\left(e_i\right) + 2\mu e_i^TA^TPBf\left(e_i\right) \\
&\quad + \mu f^T\left(e_i\right)B^TPBf\left(e_i\right) + 2c\sum_{j=1}^{N} g_{ij}e_i^TP\Gamma e_j + 2c\mu\sum_{j=1}^{N} g_{ij}e_i^TA^TP\Gamma e_j \\
&\quad + 2c\mu\sum_{j=1}^{N} g_{ij}f^T\left(e_j\right)B^TP\Gamma e_j + c^2\mu\sum_{j=1}^{N} g_{ij}e_j{}^T\Gamma^TP\Gamma\sum_{j=1}^{N} g_{ij}e_j\Bigg].
\end{aligned} \tag{16}$$

It can be obtained from Lemma 10 that

$$\begin{aligned}
&2e_i^TPBf\left(e_i\right) + 2\mu e_i^TA^TPBf\left(e_i\right) \\
&\quad \le e_i^TPBQ^{-1}B^TPe_i + f^T\left(e_j\right)Q_1f\left(e_i\right) + \mu e_i^TA^TPBQ_2^{-1}B^TPAe_i + \mu f^T\left(e_i\right)Q_2f\left(e_i\right) \\
&\quad \le e_i^T\left(PBQ^{-1}B^TP + L^TQ_1L + \mu A^TPBQ_2^{-1}B^TPA + \mu L^TQ_2L\right)e_i.
\end{aligned} \tag{17}$$

Similarly, according to condition (A_1), we have the following equation:

$$\begin{aligned}
&2c\sum_{i=1}^{N}\sum_{j=1}^{N} g_{ij}e_i^TP\Gamma e_j + 2c\mu\sum_{i=1}^{N}\sum_{j=1}^{N} g_{ij}e_i^TA^TP\Gamma e_j + 2c\mu\sum_{i=1}^{N}\sum_{j=1}^{N} g_{ij}f^T\left(e_i\right)B^TP\Gamma e_j \\
&\quad + c^2\mu\sum_{i=1}^{N}\left(\sum_{j=1}^{N} g_{ij}e_j^T\Gamma^TP\Gamma\sum_{j=1}^{N} g_{ij}e_j\right) \\
&= 2ce^T\left(G\otimes(P\Gamma)\right)e + 2c\mu e^T\left(G\otimes\left(A^TP\Gamma\right)\right)e + 2c\mu f^T(e)\left(G\otimes\left(B^TP\Gamma\right)\right)e \\
&\le ce^T\left(I_N\otimes P\right)e + ce^T\left(\left(G^TG\right)\otimes\left(\Gamma^TP\Gamma\right)\right)e + c\mu e^T\left(I_N\otimes(PA)\right)e \\
&\quad + c\mu e^T\left(\left(G^TG\right)\otimes\left(\Gamma^TA^TP\Gamma\right)\right)e + c\mu f^T(e)\left(I_N\otimes(PB)\right)f(e) \\
&\quad + c\mu e^T\left(\left(G^TG\right)\otimes\left(\Gamma^TB^TP\Gamma\right)\right)e + c^2\mu e^T\left(\left(G^TG\right)\otimes\left(\Gamma^TP\Gamma\right)\right)e \\
&\le ce^T\left(I_N\otimes P\right)e + ce^T\left(\left(\beta_1I_N\right)\otimes P\right)e + c\mu e^T\left(I_N\otimes(PA)\right)e \\
&\quad + c^2\mu e^T\left(\left(G^TG\right)\otimes\left(\Gamma^TP\Gamma\right)\right)e + c\mu e^T\left(\left(\beta_2I_N\right)\otimes\left(A^TP\right)\right)e + c\mu f^T(e)\left(I_N\otimes(PB)\right)f(e) \\
&\quad + c\mu e^T\left(\left(\beta_3I_N\right)\otimes\left(B^TP\right)\right)e + c^2\mu e^T\left(\left(\beta_1I_N\right)\otimes P\right)e \\
&\le \sum_{i=1}^{N}\left[e_i^T\left(cP + c\beta_1P + c\mu PA + c\mu\beta_2A^TP + c\mu L^TPBL + c\mu\beta_3B^TP + c^2\mu\beta_1P\right)e_i\right].
\end{aligned} \tag{18}$$

It follows from equations (16)–(18) and condition (A_2) that

$$\begin{aligned}V(t)\leq&\sum_{i=1}^{N}\big[e_i^T\big(A^TP+PA+\mu A^TPA+PBQ_1^{-1}B^TP+L^TQ_1L\\&+\mu A^TPBQ_2^{-1}B^TPA+\mu L^TQ_2L+cP+c\beta_1P+c\mu PA\\&+c\mu\beta_2A^TP+c\mu L^TPBL+c\mu\beta_3B^TP+c^2\mu\beta_1P)e_i\big]\\\leq&\,\alpha V(t).\end{aligned}\tag{19}$$

Due to $1+\mu(t)\alpha>0$ for $t\in(t_k,t_{k+1})$, by Lemma 6, it implies that

$$V(t)\leq V(t_k^+)e_\alpha(t,t_k).\tag{20}$$

Next, there are two cases for us to show that

$$V(t_{k+1})\leq V(t_k^+)e_\alpha(t_{k+1},t_k).\tag{21}$$

□

Case 12. If t_{k+1} is left-dense, then by the continuity of $V(t)$ and $e_\alpha(t,t_k)$, we have the following equation:

$$\begin{aligned}V(t_{k+1})&=\lim_{t\longrightarrow t_{k+1}^-}V(t)\leq\lim_{t\longrightarrow t_{k+1}^-}V(t_k^+)e_\alpha(t,t_k)\\&=V(t_k^+)e_\alpha(t_{k+1},t_k).\end{aligned}\tag{22}$$

Case 13. If t_{k+1} is left-scattered, then

$$\begin{aligned}V(t_{k+1})&=V(\rho(t_{k+1}))+\mu(\rho(t_{k+1}))V^\Delta(\rho(t_{k+1}))\\&\leq V(\rho(t_{k+1}))+\mu(\rho(t_{k+1}))\alpha V(\rho(t_{k+1}))\\&\leq[1+\mu(\rho(t_{k+1}))\alpha]V(\rho(t_{k+1}))\\&\leq e_\alpha(t_{k+1},\rho(t_{k+1}))V(t_k^+)e_\alpha(\rho(t_{k+1}),t_k)\\&\leq V(t_k^+)e_\alpha(t_{k+1},t_k).\end{aligned}\tag{23}$$

From Case 12 and Case 13 that equation (21) holds for $k\in\mathrm{N}$ and we can get the following equation:

$$\begin{aligned}V(t_k^+)=&\sum_{i\in N_1}e_i^T(t_k^+)Pe_i(t_k^+)+\sum_{i\in N_2}e_i^T(t_k^+)Pe_i(t_k^+)+\cdots+\sum_{i\in N_m}e_i^T(t_k^+)Pe_i(t_k^+)\\=&\sum_{i\in N_1}\big[((1+\Theta)q_1+1)^2e_i^T(t_k)Pe_i(t_k)+(1+\Theta)^2\overline{q}_1^2e_i^T(t_k-\tau_1)Pe_i(t_k-\tau_1)+2((1+\Theta)q_1+1)(1+\Theta)\overline{q}_1e_i^T(t_k)Pe_i(t_k-\tau_1)\big]\\&+\sum_{i\in N_2}\big[((1+\Theta)q_2+1)^2e_i^T(t_k)Pe_i(t_k)+(1+\Theta)^2\overline{q}_2^2e_i^T(t_k-\tau_2)Pe_i(t_k-\tau_2)+2((1+\Theta)q_2+1)(1+\Theta)\overline{q}_2e_i^T(t_k)Pe_i(t_k-\tau_2)\big]+\cdots\\&+\sum_{i\in N_m}\big[((1+\Theta)q_m+1)^2e_i^T(t_k)Pe_i(t_k)+(1+\Theta)^2\overline{q}_m^2e_i^T(t_k-\tau_m)Pe_i(t_k-\tau_m)+2((1+\Theta)q_m+1)(1+\Theta)\overline{q}_me_i^T(t_k)Pe_i(t_k-\tau_m)\big].\end{aligned}\tag{24}$$

Hence, we get the following equations:

$$\begin{aligned}V(t_k^+)\leq&\sum_{i\in N_1}\big[(1+\varepsilon_1)((1+\Theta)q_1+1)^2e_i^T(t_k)Pe_i(t_k)+\big(1+\varepsilon_1^{-1}\big)(1+\Theta)^2\overline{q}_1^2e_i^T(t_k-\tau_1)Pe_i(t_k-\tau_1)\big]\\&+\sum_{i\in N_2}\big[(1+\varepsilon_2)((1+\Theta)q_2+1)^2e_i^T(t_k)Pe_i(t_k)+\big(1+\varepsilon_2^{-1}\big)(1+\Theta)^2\overline{q}_2^2e_i^T(t_k-\tau_2)Pe_i(t_k-\tau_2)]+\cdots\\&+\sum_{i\in N_m}\big[(1+\varepsilon_m)((1+\Theta)q_m+1)^2e_i^T(t_k)Pe_i(t_k)+\big(1+\varepsilon_m^{-1}\big)(1+\Theta)^2\overline{q}_m^2e_i^T(t_k-\tau_m)Pe_i(t_k-\tau_m)\\\leq&\,d_MV(t_k)+\sum_{i=1}^{m}d_iV(t_k-\tau_i).\end{aligned}\tag{25}$$

When $t_1-\tau\in[t_0,t_1]$, we have the following equation:

$$V(t)\leq\mathrm{H}e^{-\nu(t-t_0)},t\in[t_0,t_1],\tag{26}$$

where $H = e^{\nu(t_1-t_0)}\sup_{t\in[t_0,t_1]}\{V(t)\}$.

Now, we shall show that

$$V(t)\le \mathrm{H}e^{-\nu(t-t_0)},\ t\in(t_1,\infty). \tag{27}$$

For $t\in$ (t1, t2], it follows from condition (A_3) that

$$\begin{aligned} V(t_1^+)&\le d_M V(t_1)+\sum_{i=1}^m d_i V(t_k-\tau_i)\le H d_M e^{-\upsilon(t_1-t_0)}+H\sum_{i=1}^m d_i e^{-\upsilon(t_1-\tau_i-t_0)}\\ &= H\left(d_M+\sum_{i=1}^m d_i e^{\upsilon\tau_i}\right)e^{-\upsilon(t_1-t_0)}\le H\frac{e^{-\upsilon(t_2-t_0)}}{e_\alpha(t_2,t_1)}. \end{aligned} \tag{28}$$

Together with equation (20), one can get the following equation:

$$\begin{aligned} V(t)&\le V(t_1^+)e_\alpha(t,t_1)\le H\frac{e^{-\nu(t_2-t_0)}}{e_\alpha(t_2,t)}\\ &\le He^{-\nu(t_2-t_0)}\le He^{-\nu(t-t_0)},\ t\in(t_1,t_2]. \end{aligned} \tag{29}$$

Thus, equation (27) holds for $t\in(t_1,t_2]$. Assume that equation (27) holds for $t\in(t_{\overline{n}},t_{\overline{n}+1}]$, $n\in Z_+$, which implies that equation (27) holds for $t\in(t_1,t_{\overline{n}+1}]$. Next, we claim that equation (27) holds for $t\in(t_{\overline{n}+1},t_{\overline{n}+2}]$. For each $i\in\{1,2,\cdots,m\}$, there are two cases for us to estimate $V(t_{\overline{n}+1}-\tau_i)$.

Case 14. When $t_{\overline{n}+1}-\tau_i\le t_1$, it holds that

$$V(t_{\overline{n}+1}-\tau_i)\le He^{-\nu(t_{\overline{n}+1}-\tau_i-t_0)}. \tag{30}$$

Case 15. When $t_{\overline{n}+1}-\tau_i>t_1$, there exist an integer $\eta<\overline{n}$ such that $t_{\overline{n}+1}-\tau_i\in(t_{\mathrm{n}},t_{\mathrm{n}+1}]$.

$$V(t_{\overline{n}+1}-\tau_i)\le He^{-\nu(t_{\overline{n}+1}-\tau_i-t_0)}. \tag{31}$$

Case 14 and Case 15 lead to $V(t_{\overline{n}+1}-\tau_i)\le He^{-\nu(t_{\overline{n}+1}-\tau_i-t_0)}$ which holds for all $i\in\{1,2,\cdots,m\}$. Hence, we have the following equation:

$$\begin{aligned} V(t_{\overline{n}+1}^+)&\le d_M V(t_{\overline{n}+1})+\sum_{i=1}^m d_i V(t_{\overline{n}+1}-\tau_i)\le \mathrm{H}d_M e^{-\upsilon(t_{\overline{n}+1}-t_0)}+H\sum_{i=1}^m d_i e^{-\upsilon(t_{\overline{n}+1}-\tau_i-t_0)}\\ &= H\left(d_M+\sum_{i=1}^m d_i e^{\upsilon\tau_i}\right)e^{-\upsilon(t_{\overline{n}+1}-t_0)}\le H\frac{e^{-\upsilon(t_{\overline{n}+2}-t_0)}}{e_\alpha(t_{\overline{n}+2},t_{\overline{n}+1})}. \end{aligned} \tag{32}$$

For $t\in(t_{\overline{n}+1},t_{\overline{n}+2}]$, one gets from equations (20) and (32) that

$$\begin{aligned} V(t)&\le V(t_{\overline{n}+1}^+)+e_\alpha(t_{\overline{n}+2},t_{\overline{n}+1})\le H\frac{e^{-\nu(t_{\overline{n}+2}-t_0)}}{e_\alpha(t_{\overline{n}+2},t)}\\ &= \mathrm{H}e^{-\nu(t_{\overline{n}+2}-t_0)}\le \mathrm{H}e^{-\nu(t-t_0)},\ t\in(t_{\overline{n}+1},t_{\overline{n}+2}]. \end{aligned} \tag{33}$$

Thus, equation (27) holds for $t\in(t_{\overline{n}+1},t_{\overline{n}+2}]$. Therefore, by mathematical induction that equation (27) holds for all $t\in(t_1,\infty)$. Then,

$$V(t)\le He^{-\nu(t-t_0)},\ t\in[t_0,\infty), \tag{34}$$

which implies $V(t)\longrightarrow 0$ as $t\longrightarrow\infty$, thus impulse-quantizing synchronization between system (9) and system (6) can be achieved.

Remark 16. System (7) is defined on hybrid time domains which include continuous time and discrete-time ones as its special cases. When $T=Z$, then $\mu(t)\equiv 1$ for all $t\in Z$, then (A_2) reduces to the following equation:

$$\begin{pmatrix} \Xi & PB & A^TPB\\ * & -Q_1 & 0\\ * & * & -Q_2 \end{pmatrix}\le 0, \tag{35}$$

where $\tilde{\Xi}\colon = A^TPA+L^TQ_2L+cL^TPBL+\quad c((c\beta_1+\beta_2A^T+\beta_3B^T)P+PA)$ and $\Xi\colon = A^TP+PA++c(1+\beta_1)P+L^T Q_1L+\tilde{\Xi}-\alpha P$ When T = R, then $\mu(t)\equiv 0$ for all $t\in R$, then (A_2) reduces to the following equation:

$$\begin{pmatrix} \Xi & PB\\ * & -Q_1 \end{pmatrix}\le 0, \tag{36}$$

where $\Xi: = A^T P + PA + +C(1+\beta_1)P + L^T Q_1 L - \alpha P$.

Remark 17. Compared to the existing results in [31], our delay-partitioning group strategy avoids the complexity of incorporating a mechanism such as index set D_k, which reorders the states at impulsive instants. Additionally, based on the pinning control method, we have developed a quantized impulse effect that can enhance the control effect and lower the cost. There are quantitative control strategies that just take output measurements into account, we can refer to ones in [32]. However, introducing impulse-quantizing into the hybrid domains is still a vacancy in the existing literature and this paper is to fill the vacancy.

Remark 18. For the existing methods in [37, 38], the main differences and advantages of our impulse-quantizing approach for complex networks lie in two aspects: (1) In [37, 38], their control strategies are aimed at the continuous time domain and it will become inapplicable once the state synchronization arises in mixed time domain. (2) In [37, 38], networks information can be communicated without any loss. However, the amount of data that can be transmitted per unit time in complex networks is frequently constrained. To lessen the strain on the communication channel during transmission, the quantization effect [39] is introduced in the controller in this study.

Corollary 19. *Under the condition of Theorem 11, when $\overline{q}_j = 0$, there exist some scalars $\alpha > 0, v > 0, \beta_i > 0$, $(i = 1, 2, 3)$, $\varepsilon_i (i = 1, \cdots, m)$, $P^T = P > 0, Q_1 > 0, Q_2 > 0$ that satisfy the following inequalities:*

$$(B_1): \left(G^T G\right) \otimes \left(\Gamma^T P \Gamma\right) \leq (\beta_1 I_N) \otimes P, \left(G^T G\right) \otimes \left(\Gamma^T A^T P \Gamma\right) \leq (\beta_2 I_N) \otimes \left(A^T P\right), \left(G^T G\right) \otimes \left(\Gamma^T B^T P \Gamma\right) \leq (\beta_3 I_N) \otimes \left(B^T P\right),$$
$$(B_2): \begin{pmatrix} \Xi & PB & \sqrt{\mu} A^T PB \\ * & -Q_1 & 0 \\ * & * & -Q_2 \end{pmatrix} \leq 0, \tag{37}$$

where $\tilde{\Xi}: = \mu A^T PA + \mu L^T Q_2 L + c\mu L^T PBL + c\mu \ ((c\beta_1 + \beta_2 A^T + \beta_3 B^T)P + PA)$ and $\Xi: = A^T P + PA + +c(1+\beta_1)P + L^T Q_1 L + \tilde{\Xi} - \alpha P$.

$$(B_3): d_M e^{v(t_{k+1}-t_k)} + e_\alpha (t_{k+1} - t_k) \leq 1, d_M = \max_{i\in\{1,\cdots,m\}} \left\{\left(1 + \varepsilon_i \left((1+\Theta) q_i + 1\right)^2\right\}. \tag{38}$$

Then, system (9) can achieve impulse-quantizing synchronization with system (6).

4. Numerical Simulations

In the section, we present a numerical example to illustrate the proposed results. Consider the following mixed continuous-discrete complex networks on time scale $T = \cup_{j=0}^{\infty} [0.3j, 0.3j + 0.2]$:

$$x_i^{\Delta}(t) = Ax_i(t) + Bf\left(x_i(t)\right) + c\sum_{j=1}^{3} g_{ij}\Gamma x_j(t), i = 1, 2, 3, \tag{39}$$

where $c = 0.1$, $f(x) = \tanh(x)$, and

$$A = \begin{pmatrix} 0.2 & 0.4 & 1.2 \\ 0 & 0.1 & 0.1 \\ 0.3 & 1.1 & 0.1 \end{pmatrix}, B = \begin{pmatrix} 0.5 & 0.2 & 1 \\ 0.2 & 0.4 & 0 \\ 0.1 & 0.7 & 0.2 \end{pmatrix}, G = \begin{pmatrix} -2 & 1 & 1 \\ 1 & -2 & 1 \\ 1 & 1 & -2 \end{pmatrix}. \tag{40}$$

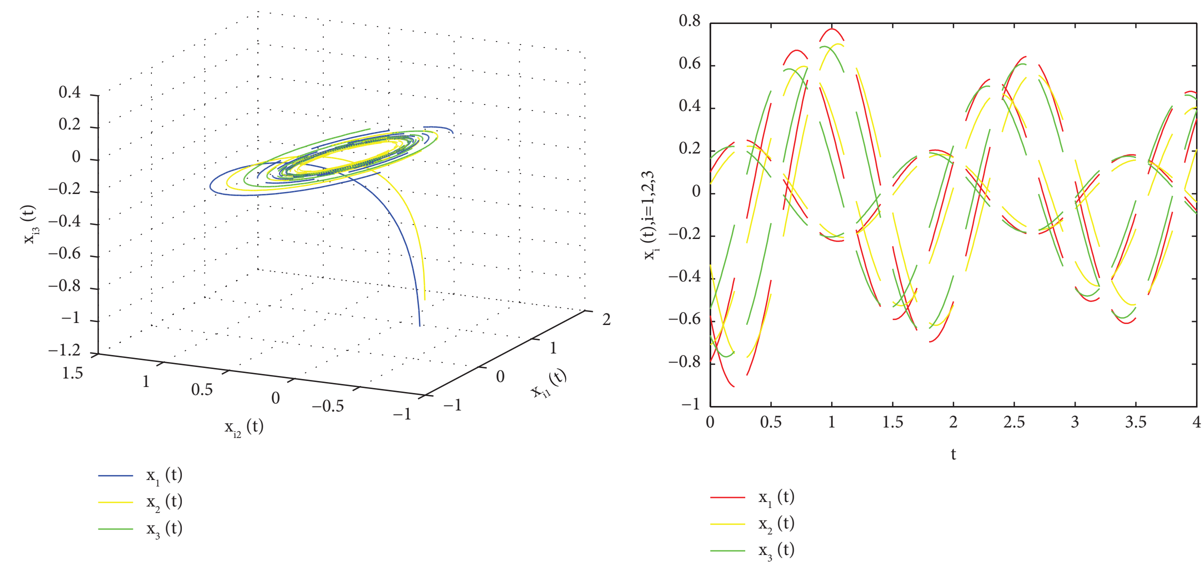

(a) (b)

Figure 1: The phase space and trajectories of $x_i(t), i = 1, 2, 3$ without impulsive control. (a) The phase space of $x_i(t), i = 1, 2, 3$. (b) The trajectories of $x_i(t), i = 1, 2, 3$.

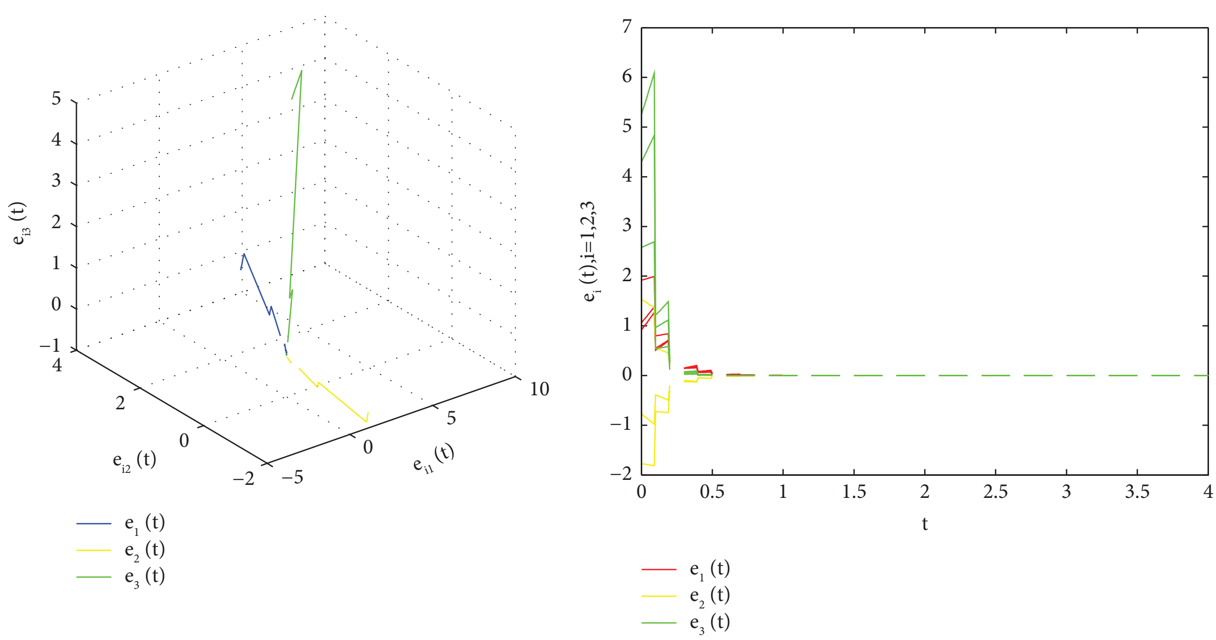

(a) (b)

Figure 2: The phase space and trajectories of $e_i(t), i = 1, 2, 3$ for Case 20. (a) The phase space of error variables. (b) The trajectories of error variables.

For the phase space and state trajectories of system (39) with initial conditions $x_1(0) = [0.25, \ -0.45, \ -1.05]^T$, $x_2(0) = [0.1, -0.55, -0.85]^T$, and $x_3(0) = [0.8, 0.15, 0.02]^T$, we can refer to Figures 1(a) and 1(b). The graininess function of T is given by the following equation:

$$\mu(t) = \begin{cases} 0, & t \in \bigcup_{j=0}^{\infty} [0.3j, 0.3j + 0.2], \\ 0.1, & t = 0.3j + 0.2, \ j \in Z^{+}, \end{cases} \tag{41}$$

which implies that $\boldsymbol{\mu}(t) \leq 0.1$ for all $\mathbf{t} \in T$.

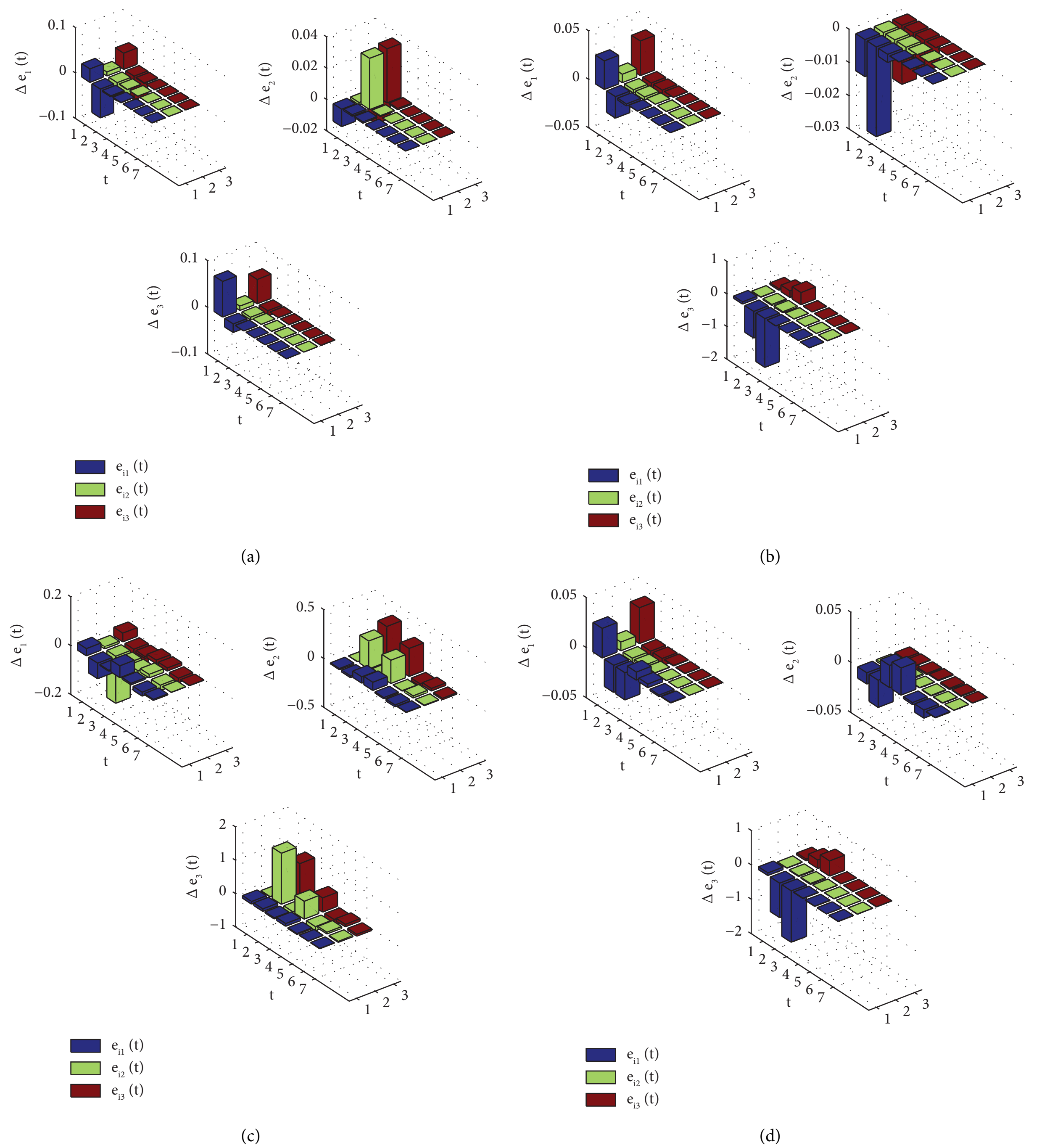

Figure 3: The impulsive effect of $e_i(t), i = 1, 2, 3$, under different impulsive controllers. (a) The impulsive magnitudes of $e_i(t)$, $i = 1, 2, 3$, for Case 20. (b) The impulsive quantized magnitudes of $e_i(t), i = 1, 2, 3$, for Case 21. (c) The impulsive magnitudes of $e_i(t)$, $i = 1, 2, 3$, for Case 22. (d) The impulsive quantized magnitudes of $e_i(t), i = 1, 2, 3$ for Case 23.

Choose $N_1 = \{1, 2\}, N_2 = \{3\}, \alpha = 3, \nu = 1, \varepsilon_i = 1 \quad (i = 1, 2)$, $m = 2$, and impulsive instants $t_k = 0.1k$, for $\mathbf{k} \in N$. It is easy to estimate the exponential function $e_\alpha(t_{k+1} - t_k) \approx 1.35$ and

$$\left(d_M + \sum_{i=1}^{m} d_i e^{\nu\tau_i} \right) e^{s(t_{k+1} - t_k)} e_\alpha(t_{k+1}, t_k) < 0.7 < 1, \tag{42}$$

which can satisfy (A_3) in Theorem 11.

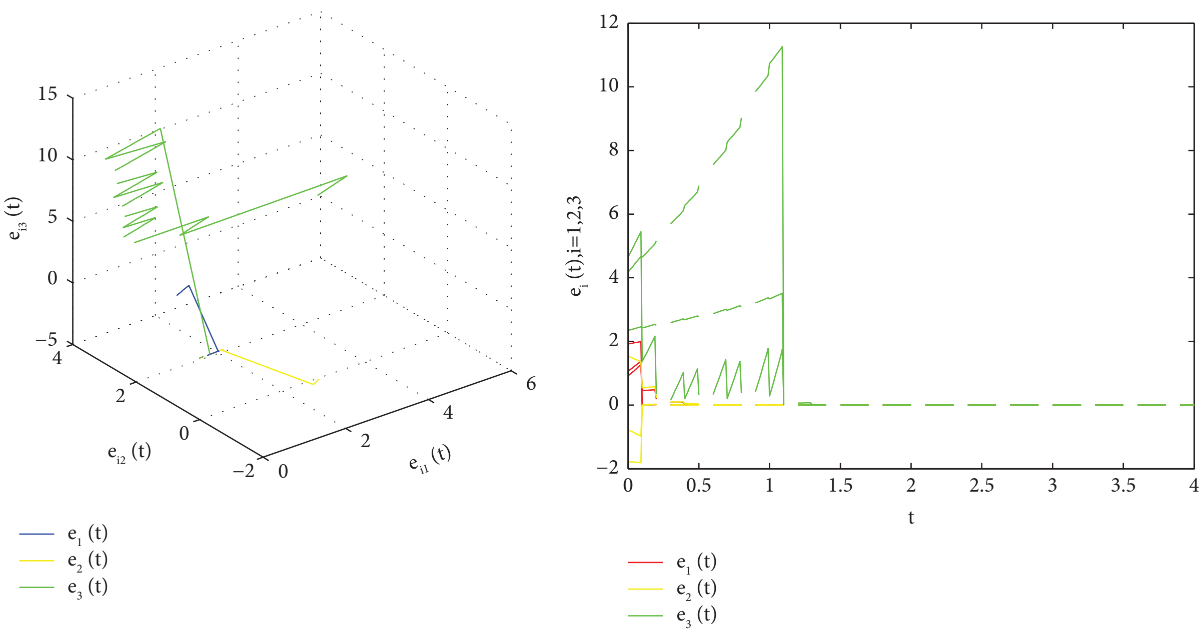

(a) (b)

Figure 4: The phase space and trajectories of $e_i(t), i = 1, 2, 3$ for Case 21. (a) The phase space of error variables. (b) The error trajectories.

Moreover, let $u_0 = 1, \delta = 0,$ and $\rho = (9/11)$; all assumptions of Theorem 11 are satisfied.

Then, the feasible solutions of LMIs in Theorem 11 can be obtained, showing that

$$P = \begin{pmatrix} 0.3282 & 0.0104 & 0.0415 \\ 0.0104 & 0.6148 & 0.1401 \\ 0.0415 & 0.01401 & 0.4438 \end{pmatrix}, Q_1 = \begin{pmatrix} 1.2586 & 0 & 0 \\ 0 & 1.2586 & 0 \\ 0 & 0 & 1.2586 \end{pmatrix}, Q_2 = \begin{pmatrix} 1.2586 & 0 & 0 \\ 0 & 1.2586 & 0 \\ 0 & 0 & 1.2586 \end{pmatrix}. \quad (43)$$

Next, consider impulsive controller as follows:

$$u_i(t) = \sum_{k=1}^{\infty} Q\left(q_j e_i(t) + \overline{q}_j e_i\left(t - \tau_j\right)\right)\delta\left(t - t_k\right), i \in N_j, \quad (44)$$

and choose $q_1 = -0.6, q_2 = -0.8, \tau_1 = 1,$ and $\tau_2 = 2$, and there are four cases for impulsive control gains.

Case 20. When $\overline{q}_1 = 0, \overline{q}_2 = 0$, and $u_i(t) = \sum_{k=1}^{\infty} q_j e_i(t) \delta(t - t_k), i \in N_j$, the error system (10) is impulsively synchronous. For phase space and trajectories of $e_i(t), i = 1, 2, 3$, we can refer to Figures 2(a) and 2(b). Figure 3(a) shows the impulsive magnitude of error variables.

Case 21. When $\overline{q}_1 = 0, \overline{q}_2 = 0$, and $u_i(t) = \sum_{k=1}^{\infty} Q (q_j e_i(t))\delta(t - t_k), i \in N_j$, the error system (10) can achieve impulse-quantizing synchronization. For phase space and trajectories of $e_i(t), i = 1, 2, 3$, we can refer to Figures 4(a) and 4(b). Figure 3(b) shows the impulsive quantized magnitude of error variables.

Case 22. When $\overline{q}_1 = -0.08, \overline{q}_2 = -0.06$, and

$$u_i(t) = \sum_{k=1}^{\infty} \left(q_j e_i(t) + \overline{q}_j e_i\left(t - \tau_j\right)\right)\delta\left(t - t_k\right), i \in N_j, \quad (45)$$

the error system (10) can achieve impulsive synchronization. For phase space and trajectories of $e_i(t), i = 1, 2, 3$, we can refer to Figures 5(a) and 5(b). Figure 3(c) shows the impulsive magnitude of error variables.

Case 23. When $\overline{q}_1 = -0.08, \overline{q}_2 = -0.06$, and

$$u_i(t) = \sum_{k=1}^{\infty} \left(Q q_j e_i(t) + \overline{q}_j e_i\left(t - \tau_j\right)\right)\delta\left(t - t_k\right), i \in N_j, \quad (46)$$

the error system (10) can achieve impulse-quantizing synchronization. For phase space and trajectories of $e_i(t), i = 1, 2, 3$, we can refer to Figures 6(a) and 6(b). Figure 3(d) shows the impulsive quantized magnitude of error variables.

Comparing Case 20 and Case 21, it can be seen from Figures 2(b) and 4(b) that the error system achieves synchronization with or without the influence of the quantization effect when delayed impulses do not exist, but the quantization increases the error magnitude. Comparing Case 22 and Case 23, it can be seen from Figures 5(a) and 6(b) that the quantization effect increases the error amplitude when delayed impulses exist, and the quantization will make the error system reach the synchronization state faster than the simple impulsive control.

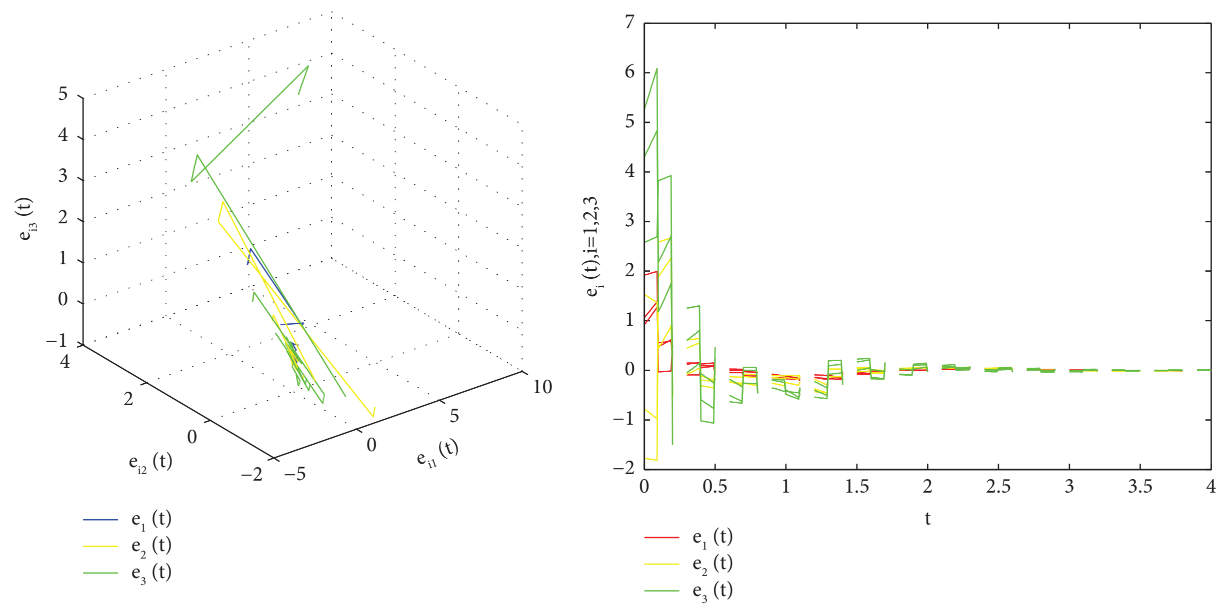

(a) (b)

FIGURE 5: The phase space and trajectories of $e_i(t), i = 1, 2, 3$, for Case 22. (a) The phase space of error variables. (b) The error trajectories.

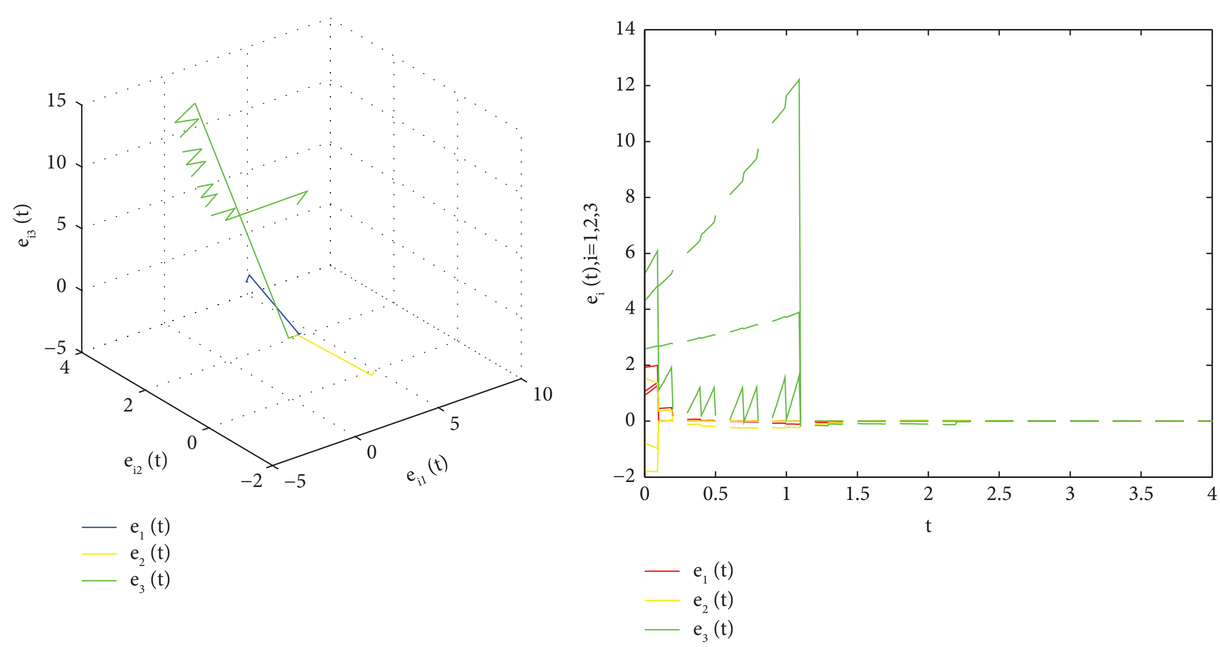

(a) (b)

FIGURE 6: The phase space and trajectories of $e_i(t), i = 1, 2, 3$, for Case 23. (a) The phase space of error variables. (b) The error trajectories.

From the above analysis, it can be seen that impulse-quantizing synchronization proposed in this paper can be achieved more economically and effectively than existing ones.

5. Conclusion

In this paper, we studied impulse-quantizing synchronization problem of mixed continuous-discrete complex networks. A delay-partitioning group-based impulsive controller which can include delays and logarithmic quantizer is designed. Multigroup pinning control and impulsive quantization can be selected to flexibly realize synchronization according to different situations. Scale-type sufficient conditions concerning the upper bound of impulses and the communication delays have been derived and analyzed. Our simulations show the interesting synchronization schemes with or without impulsive and quantized control effects.

Data Availability

The data used to support the findings of this study are available from the corresponding author upon request.

Disclosure

This paper consists of part of the preprint [34] posted on Research Square.

Conflicts of Interest

The authors declare that they have no conflicts of interest regarding this study.

References

[1] Z.-K. Gao, P.-C. Fang, M.-S. Ding, and N.-D. Jin, "Multivariate weighted complex network analysis for characterizing nonlinear dynamic behavior in two- phase flow," *Experimental Thermal and Fluid Science*, vol. 60, pp. 157–164, 2015.

[2] P. Pedro, S. D. Eppinger, and A. M. Maier, "Information flow through stages of complex engineering design projects: a dynamic network analysis approach," *IEEE Transactions on Engineering Management*, vol. 64, no. 4, pp. 604–617, 2015.

[3] Y.-H. Lan, H.-B. Gu, C.-X. Chen, Y. Zhou, and Y.-P. Luo, "An indirect Lyapunov approach to the observer-based robust control for fractional-order complex dynamic networks," *Neurocomputing*, vol. 136, no. 20, pp. 235–242, 2014.

[4] W. K. Wong, W.-B. Zhang, Y. Tang, and X.-T. Wu, "Stochastic synchronization of complex networks with mixed impulses," *IEEE Transactions on Circuits and Systems I: Regular Papers*, vol. 60, no. 10, pp. 2657–2667, 2013.

[5] S.-Q. Jiang, G.-L. Cai, S.-M. Cai, L.-X. Tian, and X.-B. Lu, "Adaptive cluster general projective synchronization of complex dynamic networks in finite time," *Communications in Nonlinear Science and Numerical Simulation*, vol. 28, no. 1-3, pp. 194–200, 2015.

[6] S.-M. Cai, P.-P. Zhou, and Z.-R. Liu, "Synchronization analysis of hybrid-coupled delayed dynamical networks with impulsive effects: a unified synchronization criterion," *Journal of the Franklin Institute*, vol. 352, no. 5, pp. 2065–2089, 2015.

[7] J.-S. Wu and L.-C. Jiao, "Synchronization in dynamic networks with nonsym- metrical time-delay coupling based on linear feedback controllers," *Physica A: Statistical Mechanics and Its Applications*, vol. 387, no. 8-9, pp. 2111–2119, 2008.

[8] J.-T. Sun, Y.-P. Zhang, F. Qiao, and Q.-D. Wu, "Some impulsive synchronization criterions for coupled chaotic systems via unidirectional linear error feedback approach," *Chaos, Solitons & Fractals*, vol. 19, no. 5, pp. 1049–1055, 2004.

[9] Y.-J. Zhang, W.-J. Yan, and Q. Yang, "Synchronization control of time-varying complex dynamic network with nonidentical nodes and coupling time-delay," *Mathematical Problems in Engineering*, vol. 2014, Article ID 461635, 8 pages, 2014.

[10] X. Wang, J.-A. Fang, A. Dai, W.-X. Cui, and G. He, "Mean square exponential synchronization for a class of Markovian switching complex networks under feedback control and M-matrix approach," *Neurocomputing*, vol. 144, no. 20, pp. 357–366, 2014.

[11] J.-Q. Lu, J. Kurths, J. D. Cao, N. Mahdavi, and C. Huang, "Synchronization control for nonlinear stochastic dynamical networks: pinning impulsive strategy," *IEEE Transactions on Neural Networks and Learning Systems*, vol. 23, no. 2, pp. 285–292, 2012.

[12] X.-F. Wang and G.-R. Chen, "Pinning control of scale-free dynamical networks," *Physica A: Statistical Mechanics and Its Applications*, vol. 310, no. 3-4, pp. 521–531, 2002.

[13] Q.-J. Zhang and J.-C. Zhao, "Projective and lag synchronization between general complex networks via impulsive control," *Nonlinear Dynamics*, vol. 67, no. 4, pp. 2519–2525, 2012.

[14] Y.-S. Lu, R.-C. Luo, and Y.-F. Zou, "Morphological analysis for three- dimensional chaotic delay neural networks," *Journal of Mathematics*, vol. 2020, no. 4, Article ID 4302505, 6 pages, 2020.

[15] Y.-Q. Li and W.-H. Jiang, "Nonlinear waves in complex oscillator network with delay," *Communications in Nonlinear Science and Numerical Simulation*, vol. 18, no. 11, pp. 3226–3237, 2013.

[16] P.-T. Gao, Y.-H. Wang, J.-X. Zhao, L.-L. Zhang, and Y. Peng, "Links syn- chronization control for the complex dynamical network," *Neurocomputing*, vol. 515, no. 1, pp. 59–67, 2023.

[17] P.-T. Gao, Y.-H. Wang, L.-Z. Liu, L.-L. Zhang, and S.-P. Li, "Double tracking control for the directed complex dynamic network via the state observer of outgoing links," *International Journal of Systems Science*, vol. 2022, no. 24, Article ID 2148495, 574 pages, 2022.

[18] Y.-P. Luo and Y.-J. Yao, "Finite-time synchronization of uncertain complex dynamic networks with time-varying delay," *Advances in Difference Equations*, vol. 2020, no. 1, pp. 32–327, 2020.

[19] F.-B. Li, P. Shi, L.-G. Wu, M. V. Basin, and C. C. Lim, "Quantized control design for cognitive radio networks modeled as nonlinear semi-markovian jump systems," *IEEE Transactions on Industrial Electronics*, vol. 62, no. 4, pp. 2330–2340, 2015.

[20] X.-H. Liu and G.-Q. Ma, "Sliding mode control for quantized semi-Markovian switching systems with bounded disturbances," *IMA Journal of Mathematical Control and Information*, vol. 36, no. 1, pp. 125–144, 2019.

[21] T. Wu, J. H. Park, L.-L. Xiong, X.-Q. Xie, and H.-Y. Zhang, "A nov- el approach to synchronization conditions for delayed chaotic Lur'e systems with state sampled-data quantized controller," *Journal of the Franklin Institute*, vol. 357, no. 14, pp. 9811–9833, 2020.

[22] L.-X. Zhang, Z.-P. Ning, and W.-X. Zheng, "Observer-based control for piecewise-affine systems with both input and output quantization," *IEEE Transactions on Automatic Control*, vol. 62, no. 11, pp. 5858–5865, 2017.

[23] J. Tao, R.-Q. Lu, H.-Y. Su, P. Shi, and Z.-G. Wu, "A synchronous filtering of nonlinear Markov jump systems with randomly occurred quantization via T-S fuzzy models," *IEEE Transactions on Fuzzy Systems*, vol. 26, no. 4, pp. 1–1877, 2017.

[24] H.-J. Gao and T.-W. Chen, "A new approach to quantized feedback control systems," *Automatica*, vol. 44, no. 2, pp. 534–542, 2008.

[25] H.-X. Rao, L.-W. Zhao, Y. Xu, Z.-H. Huang, and R. Lu, "Quasisynchronization for neural networks with partial constrained state information via intermittent control approach," *IEEE Transactions on Cybernetics*, vol. 52, no. 9, pp. 8827–8837, 2022.

[26] T.-W. Zhou, Z.-Q. Zuo, and Y.-J. Wang, "Self-triggered and event-triggered control for linear systems with quantization," *IEEE Transactions on Systems, Man, and Cybernetics: Systems*, vol. 50, no. 9, pp. 3136–3144, 2020.

[27] J. Cao, P. Li, and W.-W. Wang, "Global synchronization in arrays of delayed neural networks with constant and delayed coupling," *Physics Letters A*, vol. 353, no. 4, pp. 318–325, 2006.

[28] W.-L. Lu and T.-P. Chen, "Synchronization analysis of linearly coupled networks of discrete time systems," *Physica D: Nonlinear Phenomena*, vol. 198, no. 1-2, pp. 148–168, 2004.

[29] Q.-X. Cheng and J. Cao, "Global synchronization of complex networks with discrete time delays on time scales," *Discrete Dynamics in Nature and Society*, vol. 2011, Article ID 287670, 19 pages, 2011.

[30] Y.-X. Tan and Z.-K. Huang, "Synchronization of drive-response networks with delays on time scales," *IEEE/CAA Journal of Automatica Sinica*, vol. 2016, Article ID 7510043, 10 pages, 2017.

[31] X.-Z. Liu and K.-X. Zhang, "Synchronization of linear dynamical networks on time scales: pinning control via delayed impulses," *Automatica*, vol. 72, pp. 147–152, 2016.

[32] Y. Wan, J.-D. Cao, and G.-H. Wen, "Quantized synchronization of chaotic neural networks with scheduled output feedback control," *IEEE Transactions on Neural Networks and Learning Systems*, vol. 28, no. 11, pp. 2638–2647, 2017.

[33] Q. Xiao and Z.-G. Zeng, "Scale-limited Lagrange stability and finite-time synchronization for Memristive recurrent neural networks on time scales," *IEEE Transactions on Cybernetics*, vol. 47, no. 10, pp. 2984–2994, 2017.

[34] N. H. L.-Y. Li, B. Hong-Hua, and Z.-K. Huang, "An impulse-quantizing synchronization approach for mixed continuous-discrete complex networks," 2023, https://europepmc.org/article/ppr/ppr689087.

[35] M. Bohner and A. Peterson, *Dynamic Equations on Time Scales: An Intero- Duction with Applications*, Birkh¨auser, Boston, MA, USA, 2001.

[36] B.-L. Zhou, Y.-Q. Yang, and X.-Y. Xu, "The group-delay consensus for second- order multi-agent systems by piecewise adaptive pinning control in part of time interval," *Physica A: Statistical Mechanics and Its Applications*, vol. 513, pp. 694–708, 2019.

[37] Y.-H. Wang, W.-L. Wang, and L.-L. Zhang, "State synchronization of controlled nodes via the dynamics of links for complex dynamical networks," *Neurocomputing*, vol. 167, no. 2, pp. 429–447, 2020.

[38] P.-T. Gao, Y.-H. Wang, L.-Z. Liu, L.-L. Zhang, and X. Tang, "Asymptotical state synchronization for the controlled directed complex dynamic network via links dynamics," *Neurocomputing*, vol. 448, no. 2, pp. 60–66, 2021.

[39] Y.-X. Hong, B. Hong-Hua, and Z.-K. Huang, "Stabilization analysis of impulsive state-dependent neural networks with nonlinear disturbance: a quantization approach," *International Journal of Applied Mathematics and Computer Science*, vol. 30, no. 2, pp. 267–279, 2020.